

***In Silico* Rational Design of Ionic Liquids for Exfoliation and Dispersion of  
Boron Nitride Nanosheets**

Gregorio García,<sup>a</sup> Mert Atilhan,<sup>b</sup> and Santiago Aparicio<sup>a\*</sup>

<sup>a</sup>Department of Chemistry, University of Burgos, 09001 Burgos, Spain

<sup>b</sup>Department of Chemical Engineering, Qatar University, P.O. Box 2713, Doha, Qatar

\*Corresponding author: [sapar@ubu.es](mailto:sapar@ubu.es)

**Electronic Supplementary Information**

## THEORETICAL DETAILS

Firstly, all geometry optimizations were done using  $\omega$ B97XD functional<sup>1</sup> in combination with 6-31G(D) basis set. This functional has been selected based on two characteristics.  $\omega$ B97XD functional is a long range functional that minimize the self-interaction errors (SIE). Common DFT methods generally overestimate charge transfers.<sup>2</sup> SIE is derived from a qualitatively incorrect asymptotic potential description for the exchange correlation functional,<sup>3</sup> which is corrected through the splitting of the Coulomb repulsion energy into long-range and short-range terms.<sup>4</sup> In addition, this functional also includes dispersion corrections according to D2 Grimme's scheme.<sup>5</sup> Both dispersion interactions and charge transfer process could be adequate for a treatment of the study on the interaction between ionic liquids and boron-nitride nanosheets. In addition, calculated energies after dispersion corrections are comparable with more reliable values, such as those obtained at the MP2 level.<sup>6</sup>

Model boron nitride (BN) nanosheets were described to have a 2D honeycomb structure of 121 atoms, which was end-capped with hydrogen atoms. Smaller models have proven to be enough to study the physisorption of IL onto boron-nitride nanosheets.<sup>7</sup> Optimized nanosheet at  $\omega$ B97XD/6-31G(D) was used for further optimizations.

X-nanosheet models (X=cation or anion) were built by (randomly) placing the optimized geometry of X onto the nanosheets. For anions, those anions 1-6 were essayed, the remaining systems were obtained based on the most stable geometry of the corresponding pristine anion. For example, 3g-BN systems was built from 3-BN system. In these starting geometries, cation was placed to allow both alkyl – BN interactions or  $Z^+$  ( $Z=N^+$  for cations I-IV,  $P^+$  for V and  $S^+$  for cation VI), focusing our interest on the most stable configuration. Anions 1-6 were placed to allow a  $\pi$ -stacking between the aromatic motif and the surface with a distance of around 3.5 Å. These starting cation-BN geometries were optimized, keeping constant nanosheet coordinates. Then for each system the most geometry was fully optimized at  $\omega$ B97XD/6-31G(D) theoretical level.

After optimized starting geometries of anion-BN systems (anions 1-6) at  $\omega$ B97XD/6-31G(D), the relative disposition (through longitudinal displacements) over the surface was assessed through single point (SP) calculations. Based on these SPs, anions 1-6 were placed at the most stable disposition on BN nanosheets and the starting geometries for the remaining anions were also built. These anion-BN systems were firstly optimized in two stages: i) fixing BN coordinates; ii) fully optimization from geometries obtained in step i).

IL-BN nanosystems were optimized following a similar procedure than those described for anion-BN systems. In this case, the relative disposition between the IL and the nanosheet through longitudinal displacements was only assed for ILs based on cations IV and VI paired with anions 1g, 2g, 3g, 5g and 6i.

For IL-CO<sub>2</sub> systems, four different initial geometries (regarding to the relative disposition between CO<sub>2</sub> molecule and ionic pair were essayed), focusing our attention on the dispositions with the lowest energy. For (IL-BN)-CO<sub>2</sub> systems, we optimized an initial structure built from optimized geometries of both IL-CO<sub>2</sub> and IL-BN systems.

Based on optimized geometries, single point calculations were carried out at  $\omega$ B97XD/cc-pvDZ theoretical level, and molecular properties (such as binding energies, intermolecular interactions, atomic charge or electronic structure) obtained at this level were further used for the discussion. The Gaussian 09 (Revision D.01) package has been used for all calculations.<sup>8</sup>

Counterpoise procedure was applied to minimized basis sets superposition errors on computed binding energies.<sup>9</sup> Intermolecular interactions were featured through the analysis of the reduced density gradient (RGD) at low densities.<sup>10</sup> The visualization of RGD iso-surfaces for these peaks allows the visualization of weak interactions. The strength and the nature of the interactions is quantified through the sign of the second density Hessian eigenvalue.<sup>10</sup> Both analysis were done using MultiWFN code.<sup>11</sup> Among other available schemes, those based one on wavefuctions (e.g. Mulliken<sup>12</sup>) have been found to be very dependent the selected basis set.<sup>13</sup> Then, we selected alternative definitions of fitting atomic charges to the molecular electrostatic potentials, such as ChelpG<sup>14</sup> methods, which has proven to be suitable for describing atomic charges in ILs,<sup>15</sup> and Hirshfeld scheme which is based on the electronic density.<sup>16</sup> Total and Partial Density of States (DOS and PDOS, respectively) were calculated using GaussSum code.<sup>17</sup>

**Table 1S. Binding Energies for anion-BN interactions ( $\Delta E_{ani-BN}$ ) along to dispersion contribution to the total binding energy ( $\Delta E^D_{ani-BN}$ ) and total charge on boron nitride sheet ( $q^{BN}$ ) according to Mulliken, ChelpG and Hirshfeld populations**

Anion	$\Delta E_{ani-BN}$ / kcal mol <sup>-1</sup>	$\Delta E^D_{ani-BN}$ / kcal mol <sup>-1</sup>	$q^{BN} / e^-$		
			Mulliken	ChelpG	Hirshfeld
1	23.87	19.68	-0.204	-0.292	-0.315
1a	30.91	32.49	-0.166	-0.280	-0.346
1b	32.30	32.33	-0.169	-0.290	-0.360
1c	28.88	28.08	-0.173	-0.343	-0.310
1d	28.81	27.92	-0.169	-0.278	-0.319
1e	29.65	28.32	-0.171	-0.286	-0.332
1f	34.67	35.37	-0.163	-0.345	-0.370
1g	36.86	36.97	-0.187	-0.303	-0.396
1h	35.71	35.94	-0.177	-0.295	-0.388
1i	35.06	35.88	-0.147	-0.273	-0.354
1j	36.85	37.05	-0.163	-0.286	-0.381
2	22.51	20.86	-0.186	-0.274	-0.286
2a	30.61	33.78	-0.162	-0.271	-0.339
2b	33.84	35.05	-0.208	-0.299	-0.398
2bb	31.67	34.45	-0.178	-0.293	-0.351
2c	27.85	28.89	-0.176	-0.337	-0.310
2d	29.33	29.44	-0.176	-0.276	-0.328
2dd	28.34	29.06	-0.154	-0.269	-0.304
2e	29.25	29.77	-0.166	-0.277	-0.316
2g	37.23	38.67	-0.191	-0.299	-0.405
2h	33.55	36.96	-0.154	-0.268	-0.347
2hh	35.44	38.23	-0.159	-0.278	-0.364
2i	37.37	38.80	-0.194	-0.292	-0.400
2ii	35.93	38.35	-0.167	-0.280	-0.370
2j	34.43	37.11	-0.155	-0.282	-0.343
3	25.95	23.29	-0.176	-0.349	-0.288
3a	31.10	32.87	-0.167	-0.367	-0.349
3b	30.41	33.53	-0.189	-0.363	-0.317
3c	30.45	31.00	-0.163	-0.333	-0.303
3d	29.52	30.89	-0.148	-0.356	-0.306
3e	30.74	30.89	-0.159	-0.375	-0.321
3f	36.34	38.84	-0.156	-0.391	-0.359
3g	36.98	39.10	-0.152	-0.376	-0.366
3h	34.32	36.14	-0.153	-0.324	-0.355
3i	34.62	35.96	-0.157	-0.328	-0.365
3j	34.35	35.92	-0.146	-0.345	-0.359
4	21.23	19.05	-0.181	-0.265	-0.278
4b	32.21	31.69	-0.169	-0.277	-0.349
4c	27.88	27.67	-0.170	-0.325	-0.300
4e	28.14	27.59	-0.170	-0.274	-0.322
4f	33.33	34.45	-0.164	-0.334	-0.364
4g	34.46	35.87	-0.178	-0.280	-0.375
5	22.25	20.57	-0.178	-0.338	-0.262
5a	29.88	33.38	-0.167	-0.339	-0.323
5b	31.17	34.40	-0.195	-0.348	-0.338
5c	27.24	29.41	-0.171	-0.369	-0.282
5d	28.53	28.75	-0.174	-0.342	-0.307
5e	28.59	28.91	-0.170	-0.352	-0.312
5f	34.93	38.03	-0.180	-0.376	-0.366
5g	34.94	37.67	-0.184	-0.360	-0.364
5h	33.00	36.08	-0.153	-0.333	-0.331
5i	33.85	36.46	-0.161	-0.334	-0.337
5j	35.51	38.08	-0.183	-0.362	-0.377
6	17.83	10.82	-0.174	-0.279	-0.271
6a	27.87	24.77	-0.168	-0.288	-0.339
6d	22.84	19.61	-0.152	-0.271	-0.291
6h	29.21	28.25	-0.148	-0.278	-0.333
6i	30.11	28.31	-0.150	-0.283	-0.342

**Table 2S. Binding Energies for cation-BN interactions ( $\Delta E_{cat-BN}$ ) along to dispersion contribution to the total binding energy ( $\Delta E^D_{cat-BN}$ ) and total charge on boron nitride sheet ( $q^{BN}$ ) according to Mulliken, ChelpG and Hirshfeld populations**

Cation	$\Delta E_{cat-BN}$ / kcal mol <sup>-1</sup>	$\Delta E^D_{cat-BN}$ / kcal mol <sup>-1</sup>	$q^{BN} / e^-$		
			Mulliken	ChelpG	Hirshfeld
I	27.09	16.11	0.122	0.378	0.107
II	24.84	17.27	0.115	0.374	0.113
III	24.49	18.25	0.128	0.344	0.084
IV	22.77	13.07	0.018	0.298	0.059
V	24.92	19.18	0.126	0.346	0.100
VI	22.58	16.32	0.119	0.343	0.082

**Table 3S. Melting points,  $T_m$ , of selected ionic liquids calculated according to the method proposed by Preiss et al.<sup>18</sup>**

anion	cation	
	IV $T_m / ^\circ\text{C}$	VI $T_m / ^\circ\text{C}$
1f	58.9	19.3
1g	61.0	21.1
1h	64.3	23.7
1i	61.8	21.7
1j	58.9	19.3
2g	66.1	25.2
2hh	68.2	26.9
2i	66.8	25.8
2ii	68.9	27.5
2j	63.5	22.3
3f	63.9	21.2
3g	79.7	38.8
3h	67.7	28.7
3i	77.1	27.5
3j	72.2	23.6
5f	56.7	19.5
5g	60.2	22.4
5j	57.8	20.4
6i	17.8	-19.5

**Table 4S. Binding Energies for IL-BN interactions ( $\Delta E_{IL-BN}$ ) along to dispersion contribution to the total binding energy ( $\Delta E^D_{IL-BN}$ ) and total charge on boron nitride sheet ( $q^{BN}$ ) and both ions according to Mulliken, ChelpG and Hirshfeld populations**

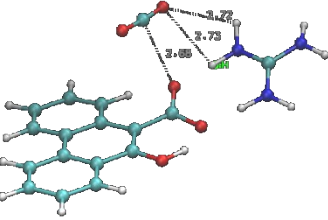
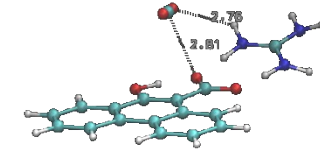
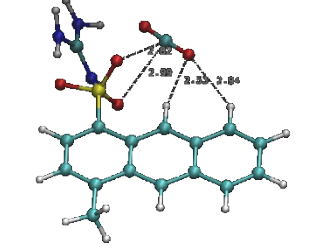
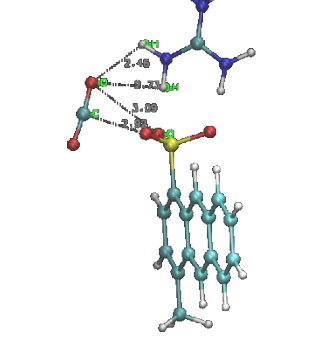
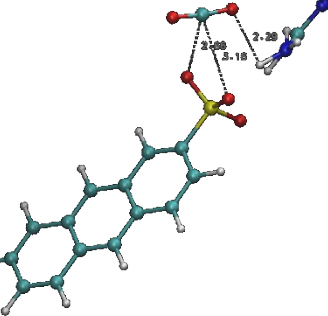
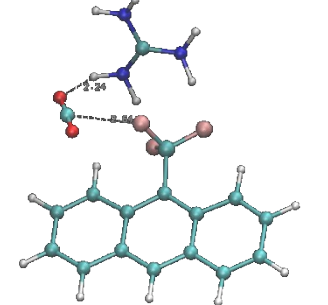
IL	$\Delta E_{ani-BN}$ / kcal mol <sup>-1</sup>	$\Delta E^D_{ani-BN}$ / kcal mol <sup>-1</sup>	$q^{BN} / e^-$		
			Mulliken	ChelpG	Hirshfeld
IV1f	37.70	44.58	-0.098	-0.081	-0.259
IV1g	40.40	46.43	-0.109	-0.044	-0.254
IV1h	38.46	45.48	-0.107	-0.052	-0.258
IV1i	38.24	45.47	-0.107	-0.053	-0.255
IV1j	40.96	46.63	-0.102	-0.046	-0.257
IV2g	42.02	47.96	-0.121	-0.053	-0.283
IV2hh	39.89	46.66	-0.125	-0.056	-0.276
IV2i	40.18	46.68	-0.124	-0.051	-0.276
IV2ii	40.60	46.84	-0.121	-0.051	-0.268
IV2j	41.67	47.73	-0.148	-0.058	-0.294
IV3f	31.94	38.28	0.005	-0.076	-0.191
IV3g	42.04	49.88	-0.119	-0.110	-0.288
IV3h	38.56	46.35	-0.122	-0.088	-0.293
IV3i	35.73	43.42	-0.101	-0.074	-0.273
IV3j	36.41	44.56	-0.057	-0.036	-0.208
IV5f	41.36	47.96	-0.137	-0.119	-0.291
IV5g	41.52	45.89	-0.088	-0.043	-0.230
IV5j	41.39	45.84	-0.089	-0.045	-0.229
IV6i	34.40	38.03	-0.112	-0.043	-0.242
VI1f	30.29	35.55	-0.061	-0.100	-0.269
VI1g	39.78	48.48	-0.022	-0.036	-0.251
VI1h	36.68	45.66	-0.034	-0.060	-0.250
VI1i	36.01	45.50	-0.036	-0.067	-0.230
VI1j	37.52	47.05	-0.033	-0.055	-0.227
VI2g	40.65	49.94	-0.039	-0.034	-0.261
VI2hh	39.63	49.87	-0.050	-0.076	-0.250
VI2i	37.69	51.65	-0.096	-0.066	-0.262
VI2ii	40.76	50.95	-0.097	-0.090	-0.275
VI2j	43.17	49.69	-0.030	-0.042	-0.240
VI3f	40.51	46.87	-0.041	-0.088	-0.236
VI3g	39.54	44.80	-0.067	-0.133	-0.271
VI3h	39.48	46.50	-0.027	-0.055	-0.251
VI3i	36.79	45.23	-0.065	-0.096	-0.269
VI3j	40.56	48.27	-0.046	-0.096	-0.264
VI5f	41.54	49.92	-0.012	-0.052	-0.219
VI5g	29.86	37.15	-0.106	-0.107	-0.185
VI5j	38.51	45.91	-0.072	-0.109	-0.255
VI6i	35.76	41.91	-0.036	-0.058	-0.259

**Table 5S. Binding Energies for cation-anion interactions ( $\Delta E_{IP}$ ) along to dispersion contribution to the total binding energy ( $\Delta E_{IP}^D$ ) and total charge on the cation ( $q^+$ ) and anion ( $q^-$ ) according to Mulliken, ChelpG and Hirshfeld populations for isolated ionic liquids as well as ionic liquids adsorbed onto the surface of BN**

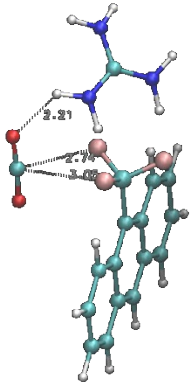
IL	Isolated Ionic Liquids					Adsorbed Ionic Liquids							
	$\Delta E_{IP}$ / kcal mol <sup>-1</sup>	$\Delta E_{IP}^D$ / kcal mol <sup>-1</sup>	$q^+ / e^-$			$\Delta E_{IP}$ / kcal mol <sup>-1</sup>	$\Delta E_{IP}^D$ / kcal mol <sup>-1</sup>	$q^+ / e^-$			$q^- / e^-$		
			Mulliken	ChelpG	Hirshfeld			Mulliken	ChelpG	Hirshfeld	Mulliken	ChelpG	Hirshfeld
IV1f	115.15	2.22	0.654	0.784	0.532	113.46	2.22	0.737	0.639	0.581	-0.639	-0.558	-0.322
IV1g	116.31	2.04	0.651	0.799	0.527	115.62	2.01	0.718	0.699	0.572	-0.609	-0.655	-0.318
IV1h	117.96	1.69	0.645	0.785	0.522	117.19	1.68	0.723	0.724	0.574	-0.616	-0.672	-0.316
IV1i	118.24	1.90	0.645	0.791	0.522	117.45	1.87	0.719	0.734	0.570	-0.612	-0.681	-0.315
IV1j	116.01	2.06	0.651	0.788	0.528	115.62	2.00	0.719	0.700	0.575	-0.617	-0.654	-0.318
IV2g	103.55	2.17	0.685	0.837	0.561	102.67	2.15	0.747	0.683	0.601	-0.626	-0.630	-0.318
IV2hh	102.44	2.07	0.676	0.808	0.553	101.74	2.05	0.750	0.731	0.600	-0.625	-0.675	-0.324
IV2ii	107.42	2.01	0.682	0.822	0.561	106.68	1.98	0.753	0.751	0.609	-0.629	-0.700	-0.333
IV2i	106.15	2.00	0.686	0.820	0.565	105.37	1.99	0.751	0.737	0.605	-0.630	-0.686	-0.337
IV2j	102.33	2.21	0.687	0.827	0.564	101.77	2.18	0.768	0.702	0.619	-0.620	-0.644	-0.325
IV3f	106.06	9.28	0.754	0.731	0.609	105.79	9.25	0.766	0.659	0.615	-0.771	-0.583	-0.424
IV3g	105.38	2.24	0.723	0.845	0.613	102.50	2.24	0.780	0.692	0.658	-0.661	-0.582	-0.370
IV3h	105.49	2.08	0.721	0.847	0.611	103.28	2.15	0.782	0.726	0.662	-0.660	-0.638	-0.369
IV3i	105.86	2.08	0.721	0.844	0.611	103.44	2.31	0.765	0.714	0.639	-0.664	-0.640	-0.366
IV3j	105.25	2.49	0.722	0.863	0.610	102.58	3.65	0.760	0.696	0.613	-0.703	-0.660	-0.405
IV5f	94.34	3.23	0.792	0.898	0.700	92.05	2.84	0.837	0.615	0.719	-0.700	-0.496	-0.428
IV5g	96.16	3.09	0.786	0.894	0.694	95.25	3.08	0.785	0.788	0.667	-0.697	-0.745	-0.437
IV5j	95.97	3.12	0.787	0.896	0.695	95.14	3.05	0.788	0.783	0.669	-0.699	-0.738	-0.440
IV6i	109.02	2.15	0.653	0.541	0.550	108.29	2.13	0.739	0.505	0.612	-0.627	-0.462	-0.370
VI1f	90.56	7.69	0.790	0.728	0.703	90.29	7.42	0.804	0.596	0.716	-0.743	-0.496	-0.447
VI1g	96.39	2.41	0.719	0.723	0.637	93.33	2.02	0.718	0.613	0.683	-0.696	-0.577	-0.432
VI1h	95.58	2.28	0.718	0.728	0.640	92.63	2.18	0.728	0.663	0.676	-0.694	-0.603	-0.426
VI1i	97.32	2.21	0.712	0.725	0.631	94.34	2.07	0.725	0.649	0.659	-0.689	-0.582	-0.429
VI1j	96.08	2.40	0.718	0.719	0.636	93.83	2.56	0.730	0.640	0.669	-0.697	-0.585	-0.442
VI2g	85.44	2.56	0.747	0.733	0.665	82.11	2.33	0.744	0.633	0.713	-0.705	-0.599	-0.452
VI2hh	83.37	2.41	0.744	0.741	0.664	80.59	3.42	0.770	0.729	0.699	-0.720	-0.653	-0.449
VI2ii	88.58	2.32	0.748	0.744	0.667	80.02	2.84	0.802	0.628	0.751	-0.706	-0.562	-0.489
VI2i	87.44	2.34	0.753	0.755	0.676	85.50	2.88	0.786	0.765	0.688	-0.689	-0.675	-0.413
VI2j	82.96	2.88	0.757	0.725	0.677	81.40	2.56	0.762	0.651	0.715	-0.732	-0.609	-0.475
VI3f	88.41	4.40	0.789	0.806	0.711	88.06	4.62	0.745	0.716	0.686	-0.704	-0.628	-0.450
VI3g	95.68	5.16	0.735	0.803	0.662	65.06	3.73	0.866	0.823	0.846	-0.799	-0.690	-0.575
VI3h	89.25	2.78	0.760	0.825	0.707	87.97	2.87	0.723	0.719	0.703	-0.696	-0.664	-0.452
VI3i	89.55	3.36	0.757	0.754	0.690	87.44	2.49	0.772	0.794	0.734	-0.707	-0.698	-0.465
VI3j	91.31	4.50	0.756	0.847	0.679	90.25	4.78	0.753	0.695	0.713	-0.707	-0.599	-0.449
VI5f	81.95	3.51	0.803	0.873	0.762	79.10	3.54	0.743	0.634	0.747	-0.731	-0.582	-0.528
VI5g	86.10	9.44	0.784	0.748	0.712	75.00	4.59	0.827	0.804	0.756	-0.721	-0.697	-0.571
VI5j	88.79	11.78	0.819	0.715	0.696	80.81	5.48	0.810	0.673	0.759	-0.738	-0.564	-0.504
VI6i	89.81	2.81	0.729	0.560	0.640	88.78	2.61	0.745	0.518	0.719	-0.709	-0.460	-0.460

<sup>a</sup> For isolated ionic liquids,  $q^- = -q^+$ .

**Table 6S. Binding Energies related to CO<sub>2</sub> capture by ILs IV2j, IV3g, IV3h and IV5f ( $\Delta E_{IL-CO_2}$ ) along optimized molecular geometries**

Ionic Liquid	Conformer	$\Delta E_{IL-CO_2}$ / kcal mol <sup>-1</sup>	Optimized Geometry
IV2j	c3	3.27	
	c4	2.98	
IV3g	c1	4.47	
	c2	5.08	
IV3h	c2	5.00	
IV5f	c1	4.52	



	c2	5.10	
--	----	------	--

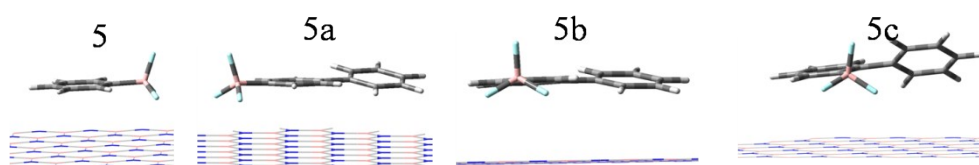


**Figure 1S.** Optimized structure of anion-BN systems, anion=5, 5a, 5b and 5c.

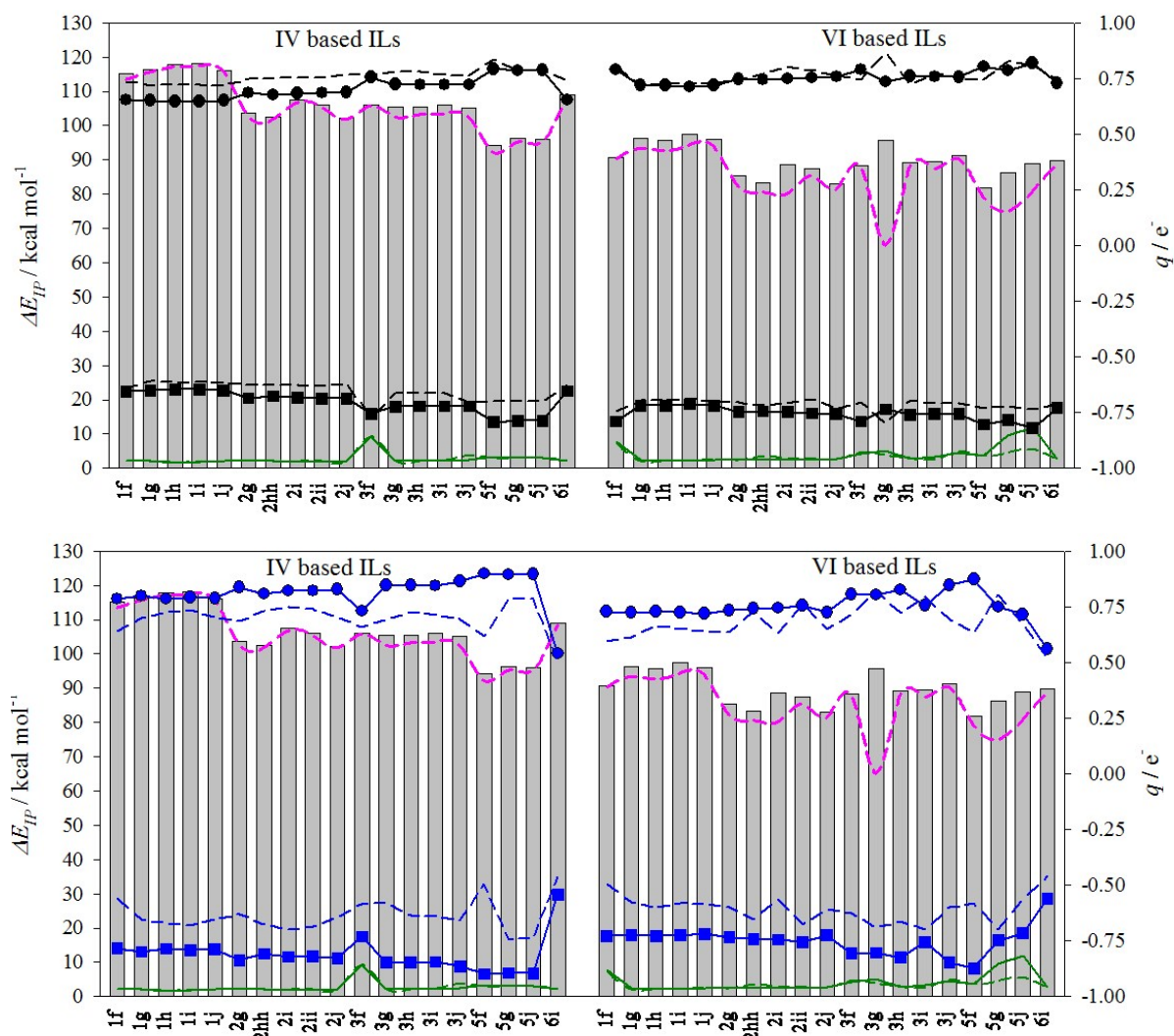


**Figure 2S.** Binding energies for cation-anion interactions ( $\Delta E_{IL}$ , grey bars and grey dotted lines for isolated IL and IL on the surface of BN, respectively) along to dispersion contribution to the total binding energy ( $\Delta E^D_{IL}$ , solid and dotted green lines for isolated IL and IL on the surface of BN, respectively) and total charge on the cation ( $q^+$ , circles) and anion ( $q^-$ , squares) according to (up) Mulliken and (bottom) ChelpG populations for isolated ionic liquids (solid lines) as well as ionic liquids adsorbed onto the surface of BN (dotted lines). Data for this Figure are in Table 4S.

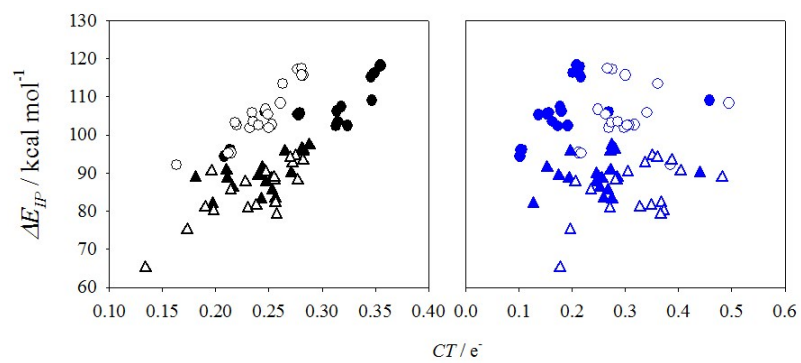


**Figure 3S.** Evolution of binding energies ( $\Delta E_{IP}$ ) for the interaction between ions as a function of the charge transfer (CT) according to Mulliken (black) and ChelpG (blue) populations. Circles / triangles correspond to IV / VI cation based ionic liquids, while filled /empty symbols stand for isolated / adsorbed ionic pairs.

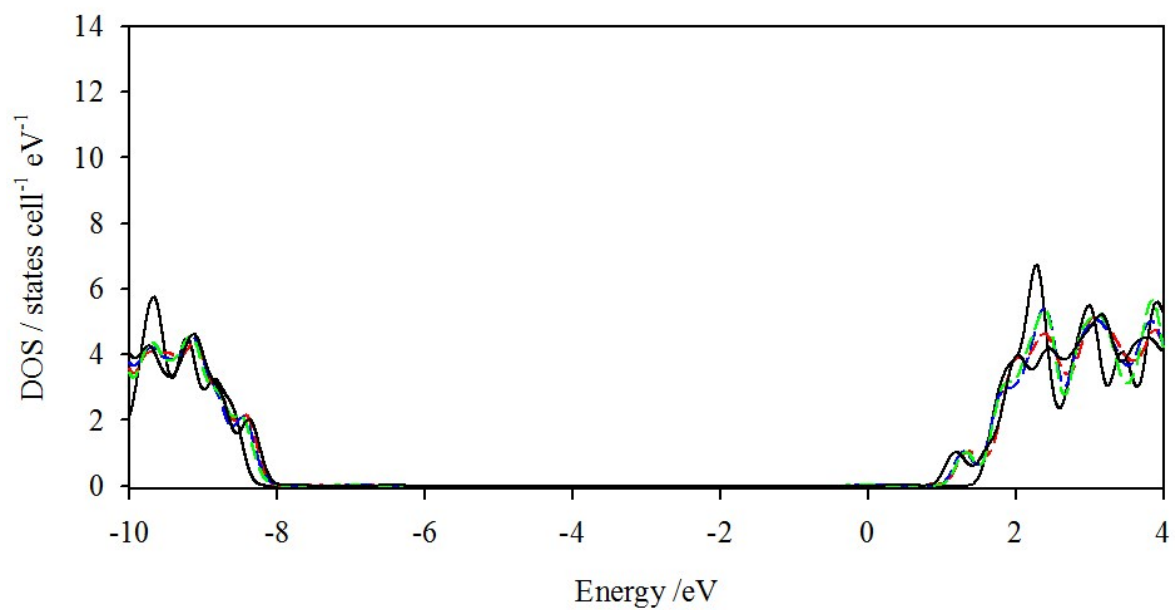


**Figure 4S.** DOS of Pristine boron-nitride nanosheet (black solid line) along to PDOS corresponding to nanosheet atoms (dotted lines) for IV2j-BN (red), IV3g-BN (blue), IV3g-BN (green) and IV5f-BN (pink) systems.

## REFERENCES

1. J.-D. Chai, M. Head-Gordon, *Phys. Chem. Chem. Phys.*, 2008, **10**, 6615-6620.
2. T. Bally, G. N. Sastry, *J. Phys. Chem. A*, 1997, **101**, 7923-7925; O. V. Gritsenko, B. Ensing, P. R. T. Schipper, E. J. Baerends, *J. Phys. Chem. A*, 2000, **104**, 8558-8565.
3. A. J. Cohen, P. Mori-Sánchez, W. Yang, *Chem. Rev.*, 2012, **112**, 289-320.
4. T. Tsuneda, K. Hirao, *Wiley Interdisciplinary Reviews: Computational Molecular Science*, 2014, **4**, 375-390.
5. S. Grimme, *J. Comput. Chem.*, 2006, **27**, 1787-1799.
6. T. Schwabe, S. Grimme, *Phys. Chem. Chem. Phys.*, 2007, **9**, 3397-3406.
7. M. Shakourian-Fard, G. Kamath, Z. Jamshidi, *J. Phys. Chem. C*, 2014, **118**, 26003-26016.
8. M. J. Frisch, G. W. Trucks, H. B. Schlegel, G. E. Scuseria, M. A. Robb, J. R. Cheeseman, G. Scalmani, V. Barone, B. Mennucci, G. A. Petersson, H. Nakatsuji, M. Caricato, X. Li, H. P. Hratchian, A. F. Izmaylov, J. Bloino, G. Zheng, J. L. Sonnenberg, M. Hada, M. Ehara, K. Toyota, R. Fukuda, J. Hasegawa, M. Ishida, T. Nakajima, Y. Honda, O. Kitao, H. Nakai, T. Vreven, J. A. Montgomery, Jr., J. E. Peralta, F. Ogliaro, M. Bearpark, J. J. Heyd, E. Brothers, K. N. Kudin, V. N. Staroverov, R. Kobayashi, J. Normand, K. Raghavachari, A. Rendell, J. C. Burant, S. S. Iyengar, J. Tomasi, M. Cossi, N. Rega, J. M. Millam, M. Klene, J. E. Knox, J. B. Cross, V. Bakken, C. Adamo, J. Jaramillo, R. Gomperts, R. E. Stratmann, O. Yazyev, A. J. Austin, R. Cammi, C. Pomelli, J. W. Ochterski, R. L. Martin, K. Morokuma, V. G. Zakrzewski, G. A. Voth, P. Salvador, J. J. Dannenberg, S. Dapprich, A. D. Daniels, Ö. Farkas, J. B. Foresman, J. V. Ortiz, J. Cioslowski, and D. J. Fox, *Gaussian 09, Revision D.01*, Gaussian, Inc.: Wallingford, CT, USA, 2009.
9. S. F. Boys, F. Bernardi, *Molecular Physics*, 1970, **19**, 553-566.
10. E. R. Johnson, S. Keinan, P. Mori-Sánchez, J. Contreras-García, A. J. Cohen, W. Yang, *J. Am. Chem. Soc.*, 2010, **132**, 6498-6506.
11. T. Lu, F. Chen, *J. Comput. Chem.*, 2012, **33**, 580-592.
12. R. S. Mulliken, *J. Chem. Phys.*, 1955, **23**, 1833.
13. J. J. Philips, M. A. Hudspeth, P. M. Browne Jr, J. E. Peralta, *Chemical Physics Letters*, 2010, **495**, 146-150.
14. C. M. Breneman, K. B. Wiberg, *J. Comput. Chem.*, 1990, **11**, 361-373.
15. S. Aparicio, M. Atilhan, *Chemical Physics*, 2012, **400**, 118-125; S. Aparicio, M. Atilhan, *Energy Fuels*, 2013, **27**, 2515-2527; V. Sanz, R. Alcalde, M. Atilhan, S. Aparicio, *J. Mol. Model.*, 2014, **20**, 1-14; S. Aparicio, M. Atilhan, *J. Chem. Phys. B*, 2012, **116**, 9171-9185; S. Aparicio, M. Atilhan, *Energy Fuels*, 2010, **24**, 4989-5001.
16. F. L. Hirshfeld, *Theoret. Chim. Acta*, 1977, **44**, 129-138.
17. N. M. O'Boyle, A. L. Tenderholt, K. M. Langner, *J. Comput. Chem.*, 2008, **29**, 839-845.
18. U. Preiss, S. Bulut, I. Krossing, *J. Phys. Chem. B* 2010, **114**, 11133-11140.